On the Expected Size of Minimum-Energy Path-preserving Topologies for Wireless Multi-hop Networks

Ashikur Rahman and Nael Abu-Ghazaleh
Department of Computer Science, Thomas J. Watson School of Engineering and Applied Science
State University of New York, P.O. Box 6000, Binghamton, NY 13902-6000
Email: {arahma, nael}@cs.binghamton.edu

***Abstract*—Topology Control (TC) algorithms for multi-hop wireless networks create a connected communication subgraph that satisfies some topological properties by assigning appropriate transmission power to each node. A topology is said to be minimum-energy path-preserving if it preserves minimum energy paths between every pair of nodes. Creating minimum-energy path-preserving sparse topologies is a fundamental research problem in TC that has been addressed in several recent research works. Although sparseness is a key metric in comparing the performance of such algorithms, none of these prior works provides analytical models to determine the sparseness. In this paper, we provide a generic analytical model for evaluating sparseness of such topologies. The derived analytical expressions are useful in determining topology size without running simulations or prior to the deployment of real systems. Moreover, we demonstrate how to analytically couple sparseness of topologies with the radio transceiver parameters. The analytical expressions are validated through extensive simulation experiments.**

I. Introduction

Topology control is a fundamental research problem for both *wired* and *wireless* networks. In a wired network, topology control refers to *twisting* the physical layout of interconnection patterns which *often* requires significant efforts from the administrator/network operator. In contrast, topology control in wireless domain is comparatively easier to achieve. By simply manipulating the transmission powers, one can easily modify underlying topologies and switch from one to another in order to meet desirable performance characteristics as needed.

On the contrary, the topology size of a wired network, once it is configured, is easy to determine. For example, a typical ring topology with n nodes contains exactly n links between them. Similarly, a (fully) mesh topology of n nodes has exactly ${}^nC_2 = \frac{n(n-1)}{2}$ links. However, determining the total number of links present in a wireless network after reconfiguring topology is a non-trivial task (unless all nodes are within the communication range of each other and form a clique). It greatly depends on the rules used for eliminating the links by the underlying topology control algorithm. Graph theory has been heavily used in the literature to study the linkage structure of the topologies generated by the algorithms. However, it is unclear how to estimate the network size using such graph theoretic approach. One inherent reason lies on the fact that most of the topology control algorithms typically generate highly complex structures which are often difficult and challenging to analyze using simple mathematical formula and the existing research efforts were only targeting simple heuristics. Unlike other research works, we provide a generalized framework for estimating topology sizes by weaving graph theoretic approach with probability theory.

Nevertheless, many principal characteristics of multi-hop wireless networks often result from the communication topology. Determining the topology size is one of the keys to understanding those characteristics. For example, the number of edges in a planar graph is at most $(3n - 6)$ [16], where n is the number of vertices. Thus, if the topology size is known apriori then it is possible to determine whether the underlying topology is planarizable or not. Moreover, some performance metrics are directly or indirectly related to the topology size. For instance, the average node degree provides a crude estimation of the level of relaying burden, contention and interference. In general, the relaying burden is inversely proportional to the average node degree whereas contention and interference experienced by a node are directly proportional to the average number of neighbors. The average node degree is determined by dividing the topology size with the number of nodes present in the network.

Many topology control algorithms have been proposed over the past decade. Among them, a special class of topology control algorithms dubbed as *minimum-energy path preserving* (**MEPP**, in short hereafter) algorithms, occupy a rich proportion of state-of-the-art topology control algorithms [4], [17], [2], [14], [12], [7], [9] for *mobile* wireless multi-hop networks. A topology is said to be MEPP if it preserves minimum energy paths between every pair of nodes while creating sparser connected subgraphs. In general, these algorithms conserve energy by replacing long distance links as much as possible with (multiple) short distance links using one or more intermediate relays. Thus, key energy savings are achieved by *shifting* long distance data communications in *space* towards short distance links. As the transmission power consumption grows at least quadratically with the distance between communicating nodes, pushing communication to shorter connections potentially saves power.

Although sparseness is a key metric in comparing the performance of all MEPP algorithms, none of the prior works provide analytical models to determine the topology size

978-14799-3360-0/14/$31.00 ©2014 IEEE

or sparseness. Therefore, in this paper we derive analytical models for evaluating sparseness of topologies generated from such algorithms. While developing the model, at first, we introduce a novel locally-defined mathematical concept dubbed as *pruning region* which is coupled with each links present in the network. We further model this pruning region based on the *rules* used in MEPP algorithms for pruning longer links. The derived analytical expressions are useful in determining topology size prior to the deployment of real systems.

A careful insight to derive analytical expressions backed-up by the simulation results find that the performance of MEPP algorithms, in terms of topology size and sparseness, strongly depends on a number of *network parameters* (node number, deployment area, and node distribution), and some other *transceiver parameters* (transmission range, radio receiver power, antenna height, and gain). Notably, with small values of transmission range and large values of radio receiver power the sparseness drops down to a large extent. It turns out that, with certain settings of transceiver parameters, MEPP algorithms are unable to prune any links at all.

The major contributions of the paper are summarized as follows: (i) we provide a generic analytical model for determining size/sparseness of the MEPP topologies, (ii) The generic model is then applied to various MEPP algorithms, (iii) for the first time in the literature, we demonstrate how to analytically couple sparseness of topologies with the radio transceiver parameters. (iv) finally, we quantitatively explore how several factors such as transceiver and network parameters affect the structural density of the topologies.

The rest of the paper is organized as follows. Section II describes related works along this direction. Section III formally shows how graph theory is used to model topologies and provides a brief description of the MEPP topology control algorithms. A generic analytical model for determining topology size, sparseness and average node degree are developed in Section IV. This generic model is then applied to MEPP graph structures in Section V. Section VI validates the analytical expressions with rigorous simulation results and presents effect of different network/transceiver parameters on structural densities. Finally, Section VII concludes the paper with the possible direction for future works.

II. Related Work

The sparsest possible topology of n nodes is the *global* minimum spanning tree (MST) containing exactly $n-1$ edges. Constructing such global MST is impractical and energy-inefficient because it needs global knowledge of the network topology. Somewhat closer to global MST is the *local* MST (LMST) proposed by Li *et al.* [5] where each node creates LMST within its neighborhood graph by assigning appropriate weight to an edge based on the necessary transmission power to reach its two ends. After constructing the LMST, each node contributes to the final topology those nodes that are its neighbors in its LMST. Although LMST can be constructed in an energy-efficient distributed manner, no analytical model is known to estimate its size or sparseness. Moreover, LMST does not preserve minimum-energy paths.

In terms of sparseness, another established solution is the Relative Neighborhood Graph (RNG) proposed by Toussaint [15] where a link $\langle s,t\rangle$ is eliminated if the distance $d(s,t)$ is greater than the distance of any other node w from s or t, i.e.: $\exists w \neq s,t : max(d(s,w),d(t,w)) < d(s,t)$.

On the other hand, Gabriel graph (GG) [3], which is a super graph of RNG, eliminates a link $\langle s,t\rangle$ if for any other node w it happens that: $\exists w \neq s,t : d^2(s,w)+d^2(t,w)) \leq d^2(s,t)$.

Milic and Malek derived analytical models for quantifying dropped edges and face sizes of RNG and GG [8]. Inspired by their work, we propose a generalized framework in this paper with the following major differences. First of all, GG and RNG are planar graphs, whereas MEPP topologies are not necessarily planar. Secondly, in GG and RNG, there always exists a non-zero pruning probability of a vertex whereas for any MEPP topology control algorithm, the pruning probability of a link might be zero for certain settings of radio transceiver parameters as we demonstrate in Section IV. Finally, we provide analytical expressions for some additional performance metrics such as average node degree and topology sizes.

Rodoplu and Meng [11] are the first to conceive the idea of MEPP topologies for mobile wireless networks. Their algorithm sets a node's transmission range much lower than the maximum while keeping the network connected and maintaining minimum energy paths between every pair of nodes. Later on, their work triggered a myriad of other research works [4], [17], [2], [14], [12], [7], [9]. Li and Halpern [4] improve their result by showing that nodes can start with a very small transmit power and incrementally search for a suitable value until all minimum energy paths are preserved. Their work produces similar results to [11], but with much lower overhead. Li and Wang [6] address the algorithmic complexity of the work in [11] and provide an algorithm with lower time complexity. Ahmed *et al.* [2] further analyze MEPP topologies and propose an improved algorithm for sparse networks. In [14] and [12], the authors incorporate fault tolerance besides preserving all minimum energy paths. However, none of these works provide any analytical models to determine the sparseness/topology size. Thus, by introducing a general framework for modeling sparseness of MEPP topologies, we seek to fill this notable gap.

III. Minimum-energy Path-preserving Topology control Algorithms

In this section we present as background the distributed algorithms for constructing MEPP graph structures. The algorithms are presented with some inessential changes to make the notation and presentation more suitable for better understanding of the proposed analytical models.

A. Graph theory to model topologies

Consider an n-node, multi-hop, ad-hoc, wireless network deployed on a two-dimensional plane. Let the set of nodes, each equipped with a radio transceiver, be denoted by $V =$

$\{t_1, t_2, \ldots, t_n\}$. Suppose the transmission power $p(t)$ of any node t is adjustable up to a maximum amount P_{max}, i.e., $0 \leq p(t) \leq P_{max}$. Such a network can be modeled as a graph $G_m = (V_m, E_m)$, with the vertex set V_m representing the nodes, and the edge set E_m defined as follows:

$$E_m = \{\langle s,t\rangle \,|(s,t) \in V \times V \wedge d(s,t) \leq R_{max}\} \quad (1)$$

where $d(s,t)$ is the distance between nodes s and t and R_{max} is the maximum distance reachable by using P_{max}. The graph G_m defined this way is a visual representation of the inherent *initial* topology (i.e. before running a topology control algorithm). We use the term *topology* and *graph* interchangeably throughout this paper.

B. Energy expenditure on a link and on a path

For estimating energy expenditure on a link, we assume the generic, two-ray, wireless channel model, where the required transmission power is a function of distance [10]. To send a message from node s to node t separated by distance $d(s,t)$ the minimum necessary power is approximated by,

$$P_{s\to t} = K \times d^{\alpha}(s,t) + c \quad (2)$$

where α (≥ 2) is the path loss factor, K is a global constant and c is the power required for processing and receiving the signal. A path in a topology is a sequence of consecutive links. Therefore, the total power consumption for transmitting over an n-length path $r = \langle v_0, v_1, \ldots, v_n\rangle$ is:

$$P_{v_0 \sim v_n} = \sum_{i=0}^{n-1} P_{v_i \to v_{i+1}} = nc + \sum_{i=0}^{n-1} K \times d^{\alpha}(v_i, v_{i+1}) \quad (3)$$

C. Minimum-energy path-preserving subgraphs

We say that a graph $G_{TC} \subseteq G_m$ is a MEPP graph or, alternatively, that it has the *minimum energy property*, if for any pair of nodes (s,t) that are connected in G_m, at least one minimum energy path between s and t in G_m also belongs to G_{TC}. MEPP graphs were first defined in [4]. Typically, many MEPP graphs can be formed from the initial graph G_m. It has been shown that the smallest of such subgraphs of G_m is the graph $G_{min} = (V, E_{min})$, where $\langle s,t\rangle \in E_{min}$ iff there is no path of length greater than 1 from s to t that costs less energy than the energy required for a direct transmission between s and t. Let $G_i = (V, E_i)$ be a subgraph of $G_m = (V, E_m)$ such that $\langle s,t\rangle \in E_i$ iff $\langle s,t\rangle \in E_m$ and there is no path of length i that requires less energy than the direct one-hop transmission between s and t. Then, G_{min} is formally defined as:

$$G_{min} = \bigcap_{i=2}^{n-1} G_i \quad (4)$$

Any subgraph G' of G has the minimum energy property iff $G' \supseteq G_{min}$. Thereby, each of $G_i \supseteq G_{min}$, for any $i = 2, 3, ..., n-1$ is a MEPP graph. A variety of MEPP graphs can be created from one- or two-hop neighbor's position information. For example, let us consider a graph $G_2^1 = (V, E_2^1)$ which is a subgraph of $G_m = (V, E_m)$ such that $\langle s,t\rangle \in E_2^1$ iff $\langle s,t\rangle \in E_m$ and there is no path of length *two* that requires less energy than the direct path between s and t.

Another MEPP graph, denoted by $G_2^2 = (V, E_2^2)$, is a subgraph of $G_m = (V, E_m)$ where $\langle s,t\rangle \in E_2^2$ iff $\langle s,t\rangle \in E_m$ and there do not exist *two or more* vertex-disjoint paths of length *two* requiring less energy than the direct path between s and t.

Both G_2^1 and G_2^2 graphs can be locally constructed if only one hop neighbors' position information is available to a node because a path of length *two* between s and t can only be created by using a neighbor r of s which is also a neighbor of t. Based on Equation 3, the minimum power required to send from s to t using an intermediate node r as a relay can be defined as:

$$P_{s\to r\to t} = P_{s\to r} + P_{r\to t} = K \times [d^{\alpha}(s,r) + d^{\alpha}(r,t)] + 2c$$

Therefore, s would use r as a relay to reach t only if:

$$P_{s\to r\to t} < P_{s\to t} \quad (5)$$

Thus, a link $\langle s,t\rangle$ is pruned from s's neighborhood in G_2^1 if there exists at least one node r satisfying Equation 5. To prune the same link in G_2^2, there must exist at least *two* such relays.

D. Algorithms to construct MEPP topologies

Consider a node s that is constructing its direct neighbors either in G_2^1 or G_2^2. At first s broadcasts a single *neighbor discovery message* (NDM) at the maximum power P_{max}. For static networks, a single episode of NDM broadcast is enough to discover all neighbors. When mobility is considered, NDM needs to be sent periodically at an interval suitably chosen based on mobility dynamics. All nodes receiving the NDM reply. While s collects the replies of its neighbors, it learns their identities and locations. The set $N_G(s)$, which starts with empty set, keeps track of all the nodes discovered in the neighborhood of s in G_m. The *relay set* $\xi_G(s,t)$ between nodes s and t records all relays between them for which the pruning criteria becomes true (i.e. includes all energy efficient relays). Initially all those sets are empty too. Whenever s receives a reply to its NDM from a node v, it updates its relay and neighbor sets by executing Algorithm 1.

Algorithm 1 $updateNeighborSet(s,v)$

```
for each w ∈ N_G(s) do
    if P_{s→v→w} < P_{s→w} then
        ξ_G(s,w) = ξ_G(s,w) ∪ {v}
    else if P_{s→w→v} < P_{s→v} then
        ξ_G(s,v) = ξ_G(s,v) ∪ {w}
    end if
    N_G(s) = N_G(s) ∪ {v}
end for
```

1) Constructing G_2^1: Two different approaches for constructing G_2^1 have been proposed in [4] and [9]. In [4], which is an improved algorithm over [11], nodes start with a very small transmit power and incrementally search for a suitable value until all minimum energy paths are preserved. On the

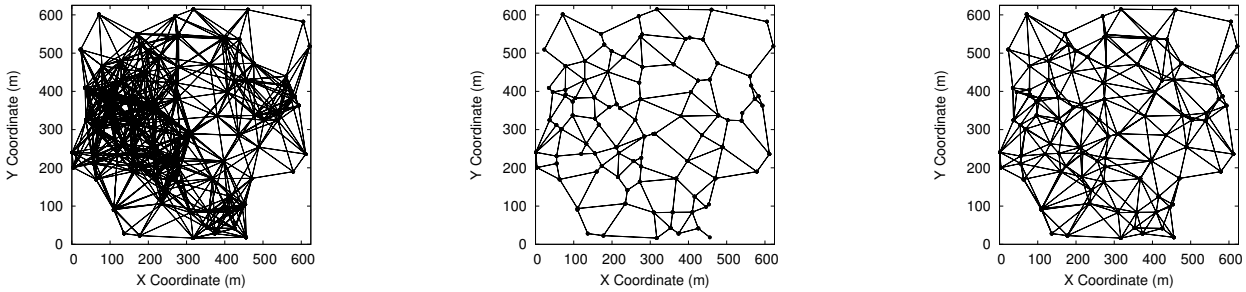

(a) Initial deployment (b) G_2^1 (c) G_2^2

Fig. 1. Illustrating an example scenario of 100 nodes deployed over a 625m × 625m square area. TX range is 150m

Algorithm 2 G_2^1 TOPOLOGY CONSTRUCTION

1: **for** each $v \in N_G(s)$ **do**
2: **if** $\xi_G(s, v)$ is empty **then**
3: $N_{G_2^1}(s) = N_{G_2^1}(s) \cup \{v\}$
4: **end if**
5: **end for**

Algorithm 3 G_2^2 TOPOLOGY CONSTRUCTION

1: **for** each $v \in N_G(s)$ **do**
2: **if** $|\xi_G(s, v)| < 2$ **then**
3: $N_{G_2^2}(s) = N_{G_2^2}(s) \cup v$
4: **end if**
5: **end for**

other hand, [9] utilizes assistance from the MAC layer for lowering the construction overhead (i.e., reducing message passing). Regardless of the approaches the inherent algorithm is the same which is described next.

After running $updateNeighborset(s, v)$, node s executes the algorithm presented in Algorithm 2 for determining its final neighbor set in G_2^1. Basically, the algorithm iteratively checks whether the relay set between s and v is empty or not. If it is empty then v is included into the neighbor set of s in G_2^1 since it indicates that there is no node that can be used as a relay to transmit message using lower energy than the direct path between s and v. Otherwise, v is excluded.

2) Constructing G_2^2: Algorithm 3 was developed by Roy at al. [12] to construct MEPP *biconnected* subgraphs, denoted by G_2^2. Assume that the algorithm is running on a node s. For each neighbor v of s in G_m the algorithm checks the number of nodes present in its relay set. If it is less than 2 then v is included into the neighbor set of s in G_2^2 since it indicates that there is at most one relay available to transmit messages using lower energy than the direct path between $s \sim v$; thus, eliminating v from its neighbor set may destroy the bi-connectivity property. Otherwise, v can be safely excluded from the final neighbor set of s in G_2^2. It has been proven that topologies constructed this way preserve minimum energy paths and ensure biconnectivity [12].

Figure 1(a) shows an example scenario of 100 nodes randomly deployed over a 625m × 625m square area. The initial topology contains 833 links in total. After running the algorithm for constructing G_2^1 the topology shown in Figure 1(b) is obtained where 74.93% links are pruned by the algorithm on an average. On the other hand the topology shown in Figure 1(c) is G_2^2 where 52.33% links are eliminated after running the corresponding topology control algorithm.

IV. GENERIC ANALYTICAL EXPRESSIONS

In this section, we provide a generic framework for determining topology size of any MEPP topology control algorithm. Suppose n nodes are uniformly spread over a deployment area A Thus, the average node density, $\mu = \frac{n}{A}$. Let us observe an arbitrary node s within this deployment area. Consider a hypothetical node t at distance x from s. Let us denote the probability of such node's existence by $P_N(x)$. Clearly $P_N(x) = 0$, if t is located outside the communication range of s. When x is located within the communication area, $P_N(x)$ can be calculated as follows. Consider a small area strip defined by dx at the perimeter of the circle with radius x and centered at s as shown in Figure 2. Also consider a small angle $d\theta$ measured from an arbitrary but fixed axis. The length of the arc $\ell = xd\theta$ and the area of the small region dA within this small strip can be approximated as, $dA = \ell dx = xdxd\theta$. Therefore, the area of the entire small strip denoted by A_{strip} becomes,

$$A_{strip} = \int_0^{2\pi} dA = \int_0^{2\pi} \ell dx = \int_0^{2\pi} xdxd\theta = 2\pi xdx$$

Thus $P_N(x)$ becomes:

$$\begin{aligned} P_N(x) &= \text{Area of the strip} \times \text{Node density} = A_{strip} \times \mu \\ &= 2\pi xdx \times \mu = 2\pi\mu xdx \end{aligned} \quad (6)$$

Once we find the probability of a node's existence at distance x, the next thing is to find the probability that a node s would *directly* communicate with such a node instead of using a relay. Obviously this communication probability depends on the topology control algorithm being used. Nevertheless, in any topology control algorithm, each node examines each link with its direct neighbors (i.e. nodes within its maximum communication range) one at a time to see whether it is possible to prune any of those links. The pruning criteria is

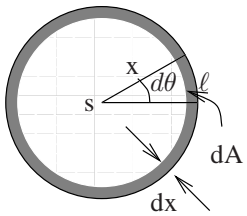

Fig. 2. Illustrating a circular strip at distance x

based on a suitably chosen *objective function* often dubbed as a "rule" in the protocol. Interestingly, for MEPP topology control algorithms, the pruning decision implicitly defines a mathematically quantifiable *pruning probability*. For example, according to the TC algorithm devised by Rodoplu et al. [11], a node is pruned if it falls within some other node's relay region (i.e. if there exist some energy-efficient node that could be used for relaying). Therefore, the pruning probability in this case is directly related to the probability of node t falling on all other node's relay region. Figure 3 provides a generic view of how a *pruning rule* translates into the *pruning probability*. Here the pruning rule implicitly defines a *pruning region* where a node's existence causes the corresponding link to be pruned. In general, the pruning probability, denoted by $P_P(x)$, is the probability that there exists a certain number of nodes inside the pruning region.

The probability of eliminating any node t from s's neighbor set, denoted by $P_E(x)$, is the probability that there exists a neighbor t at distance x from s multiplied by its pruning probability $P_P(x)$. So $P_E(x)$ becomes:

$$P_E(x) = P_N(x) \times P_P(x) = 2\pi\mu x dx \times P_P(x) \qquad (7)$$

Now, according to Equation 7, $P_E(x) = 0$, if the pruning probability $P_P(x) = 0$. Interestingly, $P_P(x)$ depends on the distance x and for low values of x it may become zero. Thus, if the distance x is small and less than certain threshold value R_L then $P_P(x)$ becomes zero. The expected number of neighbors eliminated by s from its neighbor set is found by integrating $P_E(x)$ from R_L to the maximum transmission radius R within which s possibly can communicate:

$$\mathcal{T}_e = \int_{R_L}^{R} 2\pi\mu x \times P_P(x) dx \qquad (8)$$

If we assume a disc communication area for s with radius R then the expected number of nodes within s's maximum communication range becomes $\pi R^2 \times \mu = \pi\mu R^2$. Therefore, if we divide $\mathcal{T}_e$ by $\pi\mu R^2$, we get the *average fraction of neighbors eliminated*, $\mathcal{F}_e$, which we define as *sparseness*,

$$Sparseness = \mathcal{F}_e = \frac{\mathcal{T}_e}{\pi\mu R^2} \qquad (9)$$

The average node degree is the expected number of neighbors retained after pruning. Therefore, if we subtract $\mathcal{T}_e$ from the expected number neighbors within s's communication range then we get the average node degree d_{avg}:

$$d_{avg} = \pi\mu R^2 - \mathcal{T}_e = \pi\mu R^2 - \int_{R_L}^{R} 2\pi\mu x \times P_P(x) dx \qquad (10)$$

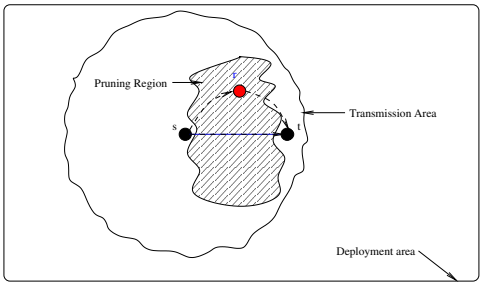

Fig. 3. Pruning probability

Finally, if we multiply d_{avg} by the total number of nodes n, we obtain twice the number of links retained after running the topology control algorithm (an edge contributes to exactly two node's degree counts). Thus, the size of the graph G_{TC} becomes,

$$\begin{aligned} S(G_{TC}) &= \frac{n \times d_{avg}}{2} = \frac{n \times \left(\pi\mu R^2 - \mathcal{T}_e\right)}{2} \\ &= \pi n\mu \left[\frac{R^2}{2} - \int_{R_L}^{R} x \times P_P(x) dx\right] \end{aligned} \qquad (11)$$

V. Sparseness of MEPP topologies

In this section we apply the generic model developed in Section IV to model MEPP topology control algorithms. For these algorithms, there exists a pruning region relative to every link such that if another node exists in the pruning region, it is more beneficial to use it as a relay than it is to use the direct link. We use geometry to derive the pruning probability from pruning rules. We apply this probability to estimate topology characteristics for G_2^1 and G_2^2 respectively.

A. Pruning probability from the pruning rule

Let us see how the *pruning rules* for constructing G_2^1 and G_2^2 can be used to derive the *pruning probability* of a link $\langle s,t\rangle$. Consider a pair of nodes (s,t). Envision the set of all points for which the pruning rule defined in Equation 5 is satisfied. This set of points collectively forms the *pruning region* of the link $\langle s,t\rangle$ and is denoted by, $\mathcal{PR}(\langle s,t\rangle)$. Mathematically,

$$\mathcal{PR}(\langle s,t\rangle) = \{\langle x,y\rangle \,|P_{s\to\langle x,y\rangle\to t} \leq P_{s\to t}\}$$

Here we use $\langle x,y\rangle$ to denote a hypothetical node located at position $\langle x,y\rangle$. The shaded region of Figure 4 shows the pruning region $\mathcal{PR}(\langle s,t\rangle)$ for path loss factor $\alpha = 2$. Any node located in this shaded area can be used as a power-saving relay and becomes one of the determining factors for eliminating the link $\langle s,t\rangle$ from the final topology. The following lemma shows an important property of the pruning regions.

Lemma 5.1: Suppose the distance between s and t is d. For $\alpha = 2$, pruning regions are circular regions centered at the midpoint on the straight line connecting s and t, and have radius $\sqrt{\frac{d^2}{4} - \frac{c}{2K}}$.

Proof: Without loss of generality, let us assume that s and t are located at $(0,0)$ and $(d,0)$. Consider a hypothetical relay node r within the pruning region of the link $\langle s,t\rangle$ positioned

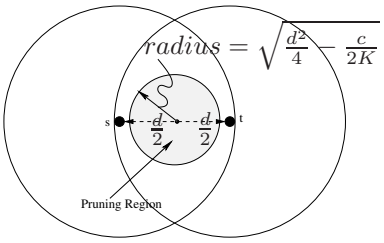

Fig. 4. Pruning region between a link $\langle s,t\rangle$

at $\langle x,y\rangle$. All nodes located inside the pruning region must satisfy the pruning criteria defined in Equation 5:

$$\begin{aligned} & P_{s\to r\to t} \le P_{s\to t} \Leftrightarrow P_{s\to r} + P_{r\to t} \le P_{s\to t} \\ \Leftrightarrow \quad & K\left[x^2+y^2+(d-x)^2+y^2\right] + 2c \le Kd^2 + c \\ \Leftrightarrow \quad & \left[x^2+y^2+(d-x)^2+y^2\right] \le d^2 - \tfrac{c}{K} \end{aligned}$$

After simplification, the expression becomes:

$$\left(x-\frac{d}{2}\right)^2 + y^2 \le \left(\sqrt{\frac{d^2}{4}-\frac{c}{2K}}\right)^2$$

which is the region confined within the circle centered at $(\frac{d}{2},0)$, and with radius $\sqrt{\frac{d^2}{4}-\frac{c}{2K}}$. Thus, any relay node capable of pruning the link $\langle s,t\rangle$ must fall within this circle. ■

When the distance d between s and t is very small such that it is lower than some threshold value, the area of the pruning region becomes zero. We can determine this threshold by setting the radius of pruning region to zero, i.e.,

$$\sqrt{\frac{d^2}{4}-\frac{c}{2K}} = 0 \Leftrightarrow d = \sqrt{\frac{2c}{K}}$$

Thus, the lower bound of transmission range becomes:

$$R_L = \sqrt{\frac{2c}{K}} \tag{12}$$

Let's find the probability that a certain number of nodes k is located within the pruning region of the link $\langle s,t\rangle$. According to Lemma 5.1 the pruning region of $\langle s,t\rangle$ link is circular region with radius $R = \sqrt{\frac{x^2}{4}-\frac{c}{2K}}$. The probability that a node is placed in this circular area πR^2 within the deployment area $A = n/\mu$ is:

$$P_\Delta = \frac{\pi R^2}{A} = \frac{\pi R^2}{\frac{n}{\mu}} = \frac{\pi\mu\left(\frac{x^2}{4}-\frac{c}{2K}\right)}{n} \tag{13}$$

The probability $P_k(\mathcal{PR}(\langle s,t\rangle))$ that exactly k nodes are located in the pruning region $\mathcal{PR}(\langle s,t\rangle)$ is:

$$P_k(\mathcal{PR}(\langle s,t\rangle)) = \binom{n-2}{k} P_\Delta^k \times (1-P_\Delta)^{n-2-k} \tag{14}$$

Note that $n-2$ is used rather than n because we exclude s and t. For large n and small P_Δ, the binomial distribution can be approximated using Poisson distribution [1], [8] with mean nP_Δ. Thus,

$$P_k\left(\mathcal{PR}(\langle s,t\rangle)\right) = \frac{(nP_\Delta)^k \times e^{-nP_\Delta}}{k!} \tag{15}$$

B. Analytical expression for G_2^1

While constructing G_2^1, a link is pruned if there exists at least *one* node inside its pruning region. Thus, the pruning probability becomes the probability that there exists one or more nodes in $\mathcal{PR}(\langle s,t\rangle)$:

$$\begin{aligned} P_P(x) &= \sum_{k=1}^{n} P_k\left(\mathcal{PR}(\langle s,t\rangle)\right) = \sum_{k=1}^{n} \frac{(nP_\Delta)^k \times e^{-nP_\Delta}}{k!} \\ &= e^{-nP_\Delta}\left(\sum_{k=0}^{\infty}\frac{(nP_\Delta)^k}{k!} - 1\right) \\ &= e^{-nP_\Delta}\left(e^{nP_\Delta}-1\right) = 1 - e^{-nP_\Delta} \end{aligned} \tag{16}$$

By substituting the value of P_Δ from Equation 13 into Equation 16, we obtain:

$$P_P(x) = 1 - e^{-\pi\mu\left(\frac{x^2}{4}-\frac{c}{2K}\right)} \tag{17}$$

By using Equation 17 and the lower bound on transmission range from Equation 12 in Equation 8 we get:

$$\begin{aligned} \mathcal{T}_e &= \int_{\sqrt{\frac{2c}{K}}}^{R} 2\pi\mu x \times P_P(x)dx \\ &= 2\pi\mu\int_{\sqrt{\frac{2c}{K}}}^{R} x\left(1 - e^{-\frac{\pi\mu x^2}{4}+\frac{\pi\mu c}{2K}}\right)dx \\ &= 2\pi\mu\int_{\sqrt{\frac{2c}{K}}}^{R} x dx - 2\pi\mu\int_{\sqrt{\frac{2c}{K}}}^{R} e^{\left(-\frac{\pi\mu x^2}{4}+\frac{\pi\mu c}{2K}\right)}dx \end{aligned}$$

After some manipulations the final expression becomes:

$$\mathcal{T}_e = \pi\mu R^2 - \frac{2\pi\mu c}{K} + 4\left[e^{\left(-\frac{\pi\mu R^2}{4}+\frac{\pi\mu c}{2K}\right)} - 1\right] \tag{18}$$

Note that, for $R < \sqrt{\frac{2c}{K}}$, no link can be pruned, thus $\mathcal{T}_e = 0$ if $R < \sqrt{\frac{2c}{K}}$. Sparseness, $\mathcal{F}_e = \mathcal{T}_e/\pi\mu R^2$. Therefore:

$$\mathcal{F}_e = \frac{1}{\pi\mu R^2}\left[\pi\mu R^2 - \frac{2\pi\mu c}{K} + 4\left\{e^{\left(-\frac{\pi\mu R^2}{4}+\frac{\pi\mu c}{2K}\right)} - 1\right\}\right] \tag{19}$$

C. Analytical expression for G_2^2

For constructing G_2^2, a link is pruned if there exists at least *two* nodes inside its pruning region. Thus, the pruning probability becomes the probability that there exists two or more nodes in $\mathcal{PR}(\langle s,t\rangle)$:

$$\begin{aligned} P_P(x) &= \sum_{k=2}^{n} P_k\left(\mathcal{PR}(\langle s,t\rangle)\right) = \sum_{k=2}^{\infty} \frac{(nP_\Delta)^k \times e^{-nP_\Delta}}{k!} \\ &= e^{-nP_\Delta}\left(\sum_{k=0}^{\infty}\frac{(nP_\Delta)^k}{k!} - \sum_{k=0}^{1}\frac{(nP_\Delta)^k}{k!}\right) \\ &= e^{-nP_\Delta}\left(e^{nP_\Delta} - 1 - nP_\Delta\right) \\ &= 1 - (nP_\Delta + 1)\, e^{-nP_\Delta} \end{aligned} \tag{20}$$

By plugging in the value of P_Δ from Equation 13 into Equation 20, we obtain:

$$P_P(x) = 1 - \left[\pi\mu\left(\frac{x^2}{4}-\frac{c}{2K}\right) + 1\right] e^{-\pi\mu\left(\frac{x^2}{4}-\frac{c}{2K}\right)} \tag{21}$$

Finally, using Equation 21 and the lower bound on transmission range from Equation 12 into Equation 8 we get:

$$\begin{aligned}\mathcal{T}_e &= \int_{\sqrt{\frac{2c}{K}}}^{R} 2\pi\mu x \times P_P(x)dx \\ &= 2\pi\mu \int_{\sqrt{\frac{2c}{K}}}^{R} x\left[1-\left(\frac{\pi\mu x^2}{4}-\frac{\pi\mu c}{2K}+1\right)e^{-\pi\mu\left(\frac{x^2}{4}-\frac{c}{2K}\right)}\right]dx \\ &= 2\pi\mu\int_{\sqrt{\frac{2c}{K}}}^{R} xdx \\ &\quad -2\pi\mu\left(1-\frac{\pi\mu c}{2k}\right)\int_{\sqrt{\frac{2c}{K}}}^{R} xe^{-\pi\mu\left(\frac{x^2}{4}-\frac{c}{2K}\right)}dx \\ &\quad -2\pi\mu\left(\frac{\pi\mu}{4}\right)\int_{\sqrt{\frac{2c}{K}}}^{R} x^3e^{-\pi\mu\left(\frac{x^2}{4}-\frac{c}{2K}\right)}dx\end{aligned}$$

The three integrals in the above equation can be separately solved as follows:

$$2\pi\mu\int_{\sqrt{\frac{2c}{K}}}^{R} xdx = 2\pi\mu\left(\frac{R^2}{2}-\frac{c}{K}\right) \tag{22}$$

$$\begin{aligned}&2\pi\mu\left(1-\frac{\pi\mu c}{2K}\right)\int_{\sqrt{\frac{2c}{K}}}^{R} xe^{-\pi\mu\left(\frac{x^2}{4}-\frac{c}{2K}\right)}dx \\ &= -4\left(1-\frac{\pi\mu c}{2K}\right)\left[e^{-\pi\mu\left(\frac{R^2}{4}-\frac{c}{2K}\right)}-1\right]\end{aligned} \tag{23}$$

and,

$$\begin{aligned}&2\pi\mu\left(\frac{\pi\mu}{4}\right)\int_{\sqrt{\frac{2c}{K}}}^{R} x^3e^{-\pi\mu\left(\frac{x^2}{4}-\frac{c}{2K}\right)}dx \\ &= 2\pi\mu\int_{\sqrt{\frac{2c}{K}}}^{R}\left(\frac{\pi\mu x^2}{4}\right)e^{-\pi\mu\left(\frac{x^2}{4}-\frac{c}{2K}\right)}xdx \\ &= 4+\frac{2\pi\mu c}{K}-\left(\pi\mu R^2+4\right)e^{-\pi\mu\left(\frac{R^2}{4}-\frac{c}{2K}\right)}\end{aligned} \tag{24}$$

Finally, using Equations 22, 23, and 24 and performing some manipulations we get:

$$\begin{aligned}\mathcal{T}_e &= \pi\mu R^2-\frac{2\pi\mu c}{K}-8 \\ &+ \left(\pi\mu R^2-\frac{2\pi\mu c}{K}+8\right)e^{-\frac{\pi\mu}{4}\left(R^2-\frac{2c}{K}\right)}\end{aligned} \tag{25}$$

Like before, $\mathcal{T}_e = 0$ if $R < \sqrt{\frac{2c}{K}}$. Sparseness, $\mathcal{F}_e = \mathcal{T}_e/\pi\mu R^2$. Therefore:

$$\begin{aligned}\mathcal{F}_e &= \frac{1}{\pi\mu R^2}\left(\pi\mu R^2-\frac{2\pi\mu c}{K}-8\right) \\ &+ \frac{1}{\pi\mu R^2}\left(\pi\mu R^2-\frac{2\pi\mu c}{K}+8\right)e^{-\frac{\pi\mu}{4}\left(R^2-\frac{2c}{K}\right)}\end{aligned} \tag{26}$$

According to Equation 19 and 26, the sparseness, $\mathcal{F}_e$ is a function of three parameters namely, maximum transmission range (R), node density (μ) and radio-receiver power (c), i.e., $\mathcal{F}_e = f(R, \mu, c)$. The general effects of these parameters (while changing one and keeping the others fixed) are as follows: $\mathcal{F}_e$ increases when either R or μ is increased, and decreases when c is increased.

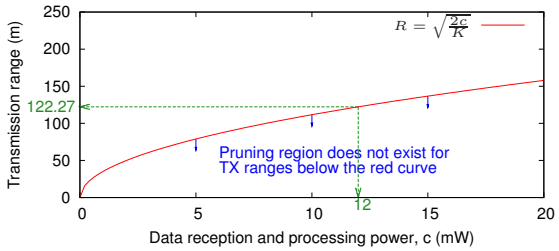

Fig. 5. Relationship between transmission range and radio-receiver power

Let us apply Equations 19 and 26 to the example scenario shown in Figure 1. The deployment area $A = 625\text{m} \times 625\text{m} = 390625$ m^2 and $n = 100$ result in a node density $\mu = n/A = 100/390625 = 0.000256$. Transmission radious $R = 150$m; suppose the receiver power $c = 0$mW. With such parameter values the Equation 19 gives us $\mathcal{F}_e = 0.781$ (i.e., 78.1%) for G_2^1 and the Equation 26 gives us $\mathcal{F}_e = 0.573$ (i.e., 57.3%) for G_2^2. Recall from Section III-D2 that the actual elimination was 74.93% for G_2^1 and 52.33% for G_2^2 which are within 5% of what we obtained using the analytical expressions.

VI. Simulation Results

In this section, we present simulation results to verify the accuracy of analytical expressions. We also explore how node density, and various transceiver parameters (transmission range and the receiver power) affect sparseness.

A. Simulation environment

1) Radio parameters: We assume that each node has an omni-directional antenna with 0 dB gain located 1.5 meter above the node. The path-loss exponent, $\alpha = 2$. The speed of light is assumed to be 3×10^8 m/sec which gives us a wavelength $\lambda = 0.001605278$m. The carrier frequency is 2.4 GHz (the operating frequency of IEEE 802.11g networks). The received signal strength threshold to ensure radio connectivity between nodes is set to -68 dBM[1]. Given these parameters, the value of K for the Equation 2 and its derivatives becomes 0.001605278 and the cross over distance becomes: $d_{cross} = \frac{4\pi h_t h_r}{\lambda} = 226.44m$. As the path loss factor α was set to 2, the *maximum* transmission range (R_{max}) was restricted below d_{cross} and set to 225m. We determine *minimum* transmission range (R_{min}) based on Equation 12. According to the equation, transmission ranges must be above $\sqrt{\frac{2c}{K}}$ in order to develop a (nonzero size) pruning region. For $R < \sqrt{\frac{2c}{K}}$, the pruning region vanishes and no power savings is possible using intermediate relays because the radio-receiver power dominates the transmit power for such a short distance communication. Therefore, R_{min} was set to $\sqrt{\frac{2c}{K}}$. As the value of K is constant for a certain set of radio parameters, R_{min} solely depends on the radio receiver power (c). However, we observe that c varies from radio to radio. With the advent of low-power circuit designs and signal processing, the receiver power of future radios is likely to be quite small. As the radio

[1]we note that commercially available LinkSys routers with WRT150N series has the similar receiver sensitivity threshold

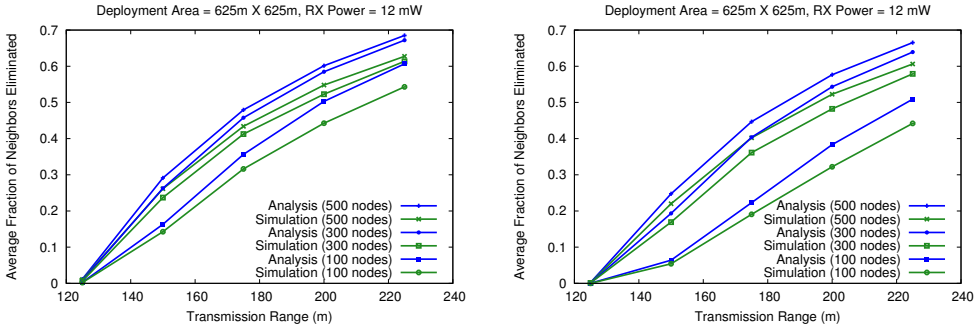

(a) G_2^1 (b) G_2^2

Fig. 6. Effect of transmission range on different graph structures.

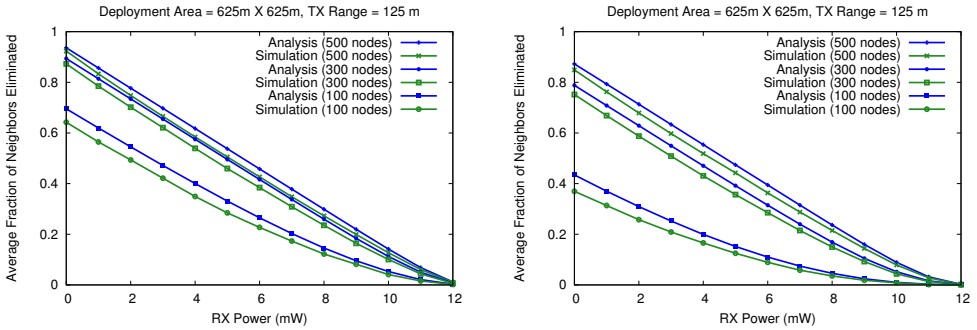

(a) G_2^1 (b) G_2^2

Fig. 7. Effect of radio-receiver power (c) on different graph structures.

receiver power (c) may have a significant impact on the size of the pruning region we decided to *vary* it to see its effect in our study. For different values of c, ranging from 0mW to 20mW, we plotted the curve $R = \sqrt{\frac{2c}{K}}$ which is shown in Figure 5. From the plot, we take 12 mW as an upper bound of c which implicitly requires the transmission range to be at least $\sim$ 122m in order to realize any power savings (i.e., to generate non-zero size pruning regions). Therefore, we set $R_{min} = 125$m, for all simulation experiments.

In short, the transmission range was varied between $R_{min} = 125$m to $R_{max} = 225$m and the radio receiver power was varied between $c_{min} = 0$mW to $c_{max} = 12$mW.

2) Scenarios: We simulate randomly deployed networks of 100, 300, and 500 nodes over a $625m \times 625m$ square region. Thus, the node density was varied by changing number of nodes over a fixed deployment region. We only consider connected networks, since it is not possible to generate *connected* MEPP sub-networks unless the initial networks are connected. For each network size we have generated 10 scenarios. Performance measures are reported as an average of these 10 random samples.

3) Performance metric: We analyze the performance of different MEPP topologies using *sparseness* as a metric. Other performance measures such as average node degree, topology size etc. are easily derivable from the sparseness (see Equations 10 and 11). The number of links remaining in a MEPP subgraph determines its sparseness. Thus, the sparseness of a network is determined by measuring the average fraction of eliminated neighbors, $\mathcal{F}_e$. The degree of sparseness of a network has a major impact on routing performance of the routing layer. For instance, *flooding*, if used for route discovery, is known to create serious *broadcast storm problem* in a dense graph [13]. By reducing neighbor set of each node, this problem can be mitigated to some extent.

B. Effect of transmission range

To see the effect of transmission range on sparseness, we measure $\mathcal{F}_e$ for both G_2^1, and G_2^2 with different node densities. The transmission range is varied between 125m to 225m with an increment of 25m at each step. Figure 6 shows the result. The power consumption of the radio receiver is set to 12mW. Measurements from both simulation experiments and analytical expressions are plotted in the same graph for a fair comparison. For both G_2^1 and G_2^2, $\mathcal{F}_e$ exponentially increases with the increase in transmission range. Moreover, G_2^1 structures prune more neighbors compared to G_2^2 structures. With $c = 12mW$, and $K = 0.001605278$ the critical transmission range becomes $R_{min} = \sqrt{\frac{2c}{K}} \cong 122m$. Therefore, $\mathcal{F}_e$ drops down to zero at 125m transmission range for both of the plots.

Figure 6(a) and 6(b) show that for all scenarios, the results of analytical expressions are very close to the simulation results; the difference is very small, maximal being around 6.5%. Thus, the analytical models are effectively able to capture the generic pattern of the simulation results. The small inaccuracy arises from the nodes located close to the boundaries of the deployment region, for which the communication area is restricted, and thus they have fewer neighbors. With larger transmission ranges the effect also becomes larger. We ignored

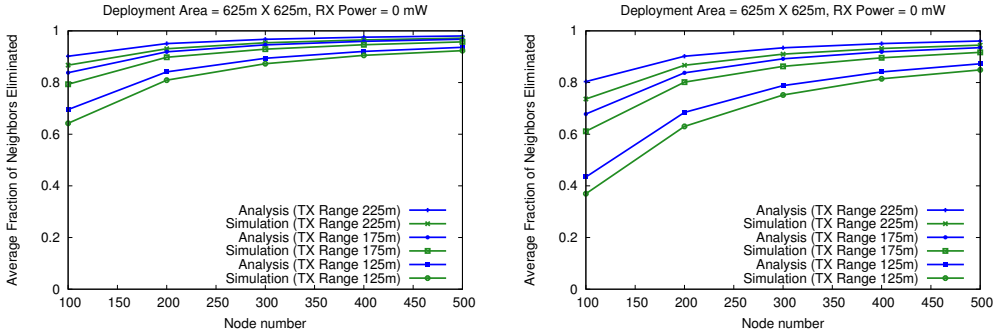

(a) G_2^1 (b) G_2^2

Fig. 8. Effect of node density on different graph structures.

this "boundary effects" to simplify the analytical models.

C. Effect of radio-receiver power (c)

Next, we explore the effect of radio-receiver power (c) on the sparseness. For different values of c, we plotted $\mathcal{F}_e$ in Figure 7 for both G_2^1, and G_2^2 graph structures with various node densities. The transmission range is set to 125m. With this transmission range the sparseness drops down to zero at $c = KR^2/2 = \left(0.001605278 \times 125^2\right)/2 \cong 12mW$. For other values of radio-receiver power, $\mathcal{F}_e$ exponentially increases with the decrease in the value of c. Moreover, G_2^1 graph structures are sparser compared to G_2^2 graph structures for any node density.

D. Effect of node density

Finally, we present the effect of node density on the sparseness. Node density were varied by varying number of nodes between $100-500$ while keeping the deployment region constant. Moreover, we have deliberately set the radio-receiver power to zero to see what happens if we ignore the receiving costs c. Figure 8(a) and 8(b) show the sparseness for both G_2^1, and G_2^2 under three transmission radius 225m, 175m and 125m. The result is as expected: a higher fraction of neighbors is eliminated in more dense networks for all transmission ranges. With larger node densities, it is highly probable that the required number of nodes exist in the pruning region of a link, and the link gets pruned by the algorithm. Unlike other plots, a rich proportion of neighbors are eliminated even for 125m transmission range. The reason is, for $c = 0$, the minimum transmission range becomes, $R_{min} = \sqrt{\frac{2c}{K}} = 0m$; consequently, for all nonzero transmission ranges, the pruning region exists and we get a nonzero value of the sparseness.

VII. Conclusions and Future Work

MEPP algorithms constitute an important class of topology control protocols for mobile wireless multi-hop networks. This class of algorithms is very appealing, practically implementable algorithms due to their simplicity, distributed property, and strictly local behavior. We provided analytical models to determine the structural densities for this class of protocols. Using the proposed models, the network designer can easily estimate the sparseness and network size for the desired topology, perhaps prior to network deployment.

There still remain some open questions to answer. The analytical expressions are developed under uniform node distributions, extending the model for other node distributions is an immediate possibility. It still remains open whether it is possible to generalize the proposed models to cover other class of topology control algorithms.

Acknowledgement

This publication was made possible by the support of the NPRP grant 08-562-1-095 from the Qatar National Research Fund. The statements made herein are solely the responsibility of the authors.

References

[1] Poisson distribution. http://en.wikipedia.org/wiki/Poisson_distribution.
[2] M. Ahmed, M. Shariar, S. Zerin, and A. Rahman. Analysis of minimum-energy path-preserving graphs for ad-hoc wireless networks. In *Symp. on Perform. Eval. of Comp. and Telecomm. Sys.*, June 2008.
[3] K. R. Gabriel and R. R. Sokal. A new statistical approach to geographic variation analysis. *Systematic Zoology*, 18(3):259–270, 1969.
[4] L. Li and J. Y. Halpern. A minimum-energy path-preserving topology-control algorithm. *IEEE Trans. on Wire. Comm.*, 3(3):910–921, 2004.
[5] N. Li, J. C. Hou, and L. Sha. Design and analysis of an MST-based topology control algorithm. In *Proceedings of INFOCOM*, 2003.
[6] X. Li and P. Wan. Constructing minimum energy mobile wireless networks. In *Proceedings of ACM MobiHoc*, pages 55–67, 2001.
[7] J. Lin, X. Zhou, and Y. Li. A minimum-energy path-preserving topology control algorithm for wireless sensor networks. *International Journal of Automation and Comp.*, 6:295–300, 2009.
[8] B. Milic and M. Malek. Dropped edges and faces' size in gabriel and relative neighborhood graphs. *IEEE MASS*, 0:407–416, 2006.
[9] A. Rahman and P. Gburzynski. MAC-assisted topology control for ad-hoc wireless networks. *Int. J. Commun. Syst.*, 19(9):955–976, 2006.
[10] T. Rappaport. Wireless communications: principles and practice, 1996.
[11] V. Rodoplu and T. Meng. Minimum energy mobile wireless networks. *IEEE Journal on Sel. Areas in Comm. (JSAC)*, 17(8):1333–1344, 1999.
[12] H. Roy, S. K. De, M. Maniruzzaman, and A. Rahman. Fault-tolerant power-aware topology control for ad hoc wireless networks. In *IFIP NETWORKING*, 2010.
[13] Y.-S. C. h. S.-Y. Ni, Y.-C. Tseng and J.-P. Sheu. The broadcast storm problem in a mobile ad hoc network. In *Mobicom*, 1999.
[14] Z. Shen, Y. Chang, C. Cui, and X. Zhang. A fault tolerant and minimum-energy path-preserving topology control algorithm for wireless multi-hop networks. In *Comp. Intell. and Sec. (CIS)*, 2005.
[15] G. Toussaint. The relative neighborhood graph of a finite planar set. *Pattern Recognition*, 12:261–268, 1980.
[16] D. B. West. *Introduction to Graph Theory*. Prentice Hall, 2000.
[17] X. Zhou, Y. Li, W. Zhao, Z. Liu, and Q. Chen. MPTC–a minimum energy path-preserving topology control algorithm for wireless sensor networks. In *Real-Time Mobile Multimedia Services*, 2007.